Reactivity and Catalytic Activity of Heteronuclear Clusters. 1. Fluxional Decapping of the Heterometallic Moiety in $H_3Ru_4(CO)_{12}MPR_3$ (M = Au, Cu) and the Crystal Structure of $H_3Ru_4(CO)_{12}AuPPh_3$

John Evans,* Andrew C. Street, and Michael Webster

Department of Chemistry, The University, Southampton SO9 5NH, U.K.

Received August 11, 1986

IR and variable-temperature ^1H and ^{31}P NMR studies have indicated that the PR_3-promoted dissociation of a copper site from $H_3Ru_4(CO)_{12}CuPR_3$ to form $[Cu(PR_3)_3]^+[H_3Ru_4(CO)_{12}]^-$ occurs as a fluxional process. The equilibrium and rate constants for the process at 285 K have been estimated for $H_3Ru_4(CO)_{12}CuPPh_3$ as 1300 M^{-2} and 30 s^{-1}, respectively, and for $H_3Ru_4(CO)_{12}CuP(p\text{-}MeC_6H_4)_3$ as 174 M^{-2} and 30 s^{-1}, respectively, at cluster and phosphine concentrations of 0.029 M. Increasing the steric bulk of the phosphine to that of $P(o\text{-}MeC_6H_4)_3$ retards the intermolecular exchange process as does the change in the heterometal atom from copper to gold. The X-ray structure of $H_3Ru_4(CO)_{12}AuPPh_3$ is reported: the compound crystallizes in the triclinic system, space group $P\bar{1}$, $Z = 2$, with cell dimensions $a = 9.428$ (1) Å, $b = 11.718$ (2) Å, $c = 17.230$ (1) Å, $\alpha = 107.36$ (9)°, $\beta = 105.52$ (1)°, and $\gamma = 89.84$ (1)°; $R = 0.0347$ from 5326 reflections ($F > 3\sigma(F)$). An approximately tetrahedral Ru_4 cluster has an edge-bridged $AuPPh_3$ grouping (Ru–Au = 2.809 (1), 2.723 (1) Å; Au–P = 2.305 (2) Å). There are two edge-bridging (μ_2-H) hydride atoms and one face-bridging (μ_3-H) hydride atom; the gold atom is not involved in hydride coordination.

Introduction

Heterogeneous bimetallic catalysts of a group 8 and a group 11d metal have been well documented.[1] In particular the activity, selectivity, and stability of a dispersed ruthenium catalyst is strongly influenced by addition of copper. Recent interest in the synthesis of heteronuclear transition-metal clusters[2-4] has provided examples of related series of clusters to probe such modifications at a molecular level in homogeneous systems. The modification of catalytic activity in heterometallic clusters is suggested by differentiated heterosite activity in $Ru_2Co_2(CO)_{13}$ that undergoes two metal specific reactions under mild conditions. Indeed, a preliminary communication from our group reported the activation toward alkene isomerization of a ruthenium cluster by a gold center.[5] Recently, considerable efforts have been directed toward the synthesis and structural elucidation of ruthenium clusters containing the heterometallic moiety $[MPPh_3]$ where M is a group 11d element.[6-17]

Table I. Crystal and Data Collection Parameters for $H_3Ru_4(CO)_{12}AuPPh_3$

mol formula	$C_{30}H_{18}AuO_{12}PRu_4$
fw	1202.7
cryst system	triclinic
space group	$P\bar{1}$ (No. 2)
a, Å	9.428 (1)
b, Å	11.718 (2)
c, Å	17.230 (1)
α, deg	107.36 (9)
β, deg	105.52 (1)
γ, deg	89.84 (1)
V, Å^3	1744.4
Z	2
ρ(calcd), g cm^{-3}	2.289
ρ(obsd), g cm^{-3}	2.30 (2) (flotation)
μ(Mo Kα), cm^{-1}	59.1
F(000)	1128
radiatn	Mo Kα (λ = 0.7107 Å)
θ range, deg	1.5 (min), 25.0 (max)
data collected	$\pm h$ (-11 to +11),k (0-13),$\pm l$ (-20 to +20)
no. of total data	6449
no. of unique data	6118
no. of obsd data ($F > 3\sigma(F)$)	5326
R^a	0.0347
$R_w{}^b$	0.0415
w	$1/[\sigma^2(F) + 0.000\,05F^2]$

$^a R = \sum(||F_o| - |F_c||)/\sum(F_o)$. $^b R_w = [\sum w(|F_o| - |F_c|)^2/\sum w(F_o)^2]^{1/2}$.

This is the first in a series of publications on the chemistry of the clusters $H_3Ru_4(CO)_{12}MPR_3$ (M = Au, Ag, Cu). The dependence of the catalytic activity and selectivity upon the heterometallic moiety in the homogeneous isomerization of alkenes has been investigated, as have the mechanistic features of the catalysis. Kinetic studies of substitution reactions in the bimetallic systems have been compared with investigations of such processes in homometallic ruthenium clusters. In this first paper, we report an X-ray crystallographic study of $H_3Ru_4(CO)_{12}AuPPh_3$ (1) and describe the phosphine-promoted decapping of this and the clusters $H_3Ru_4(CO)_{12}CuPR_3$ (2).

Experimental Section

Infrared (IR) spectra were recorded on a Perkin-Elmer PE580B spectrophotometer with Model 3500 data station. ^1H NMR spectra were obtained on Bruker AM-360 and Varian XL-100

(1) Sinfelt, J. H., *Bimetallic Catalysts*; Wiley: New York, 1983.
(2) Vahrenkamp, H. *Philos. Trans. R. Soc. London, Ser. A* **1982**, *308*, 17.
(3) Stone, F. G. A. *Philos. Trans. R. Soc. London, Ser. A* **1982**, *308*, 87.
(4) Roberts, D. A.; Geoffroy, G. L. In *Comprehensive Organometallic Chemistry*; Pergamon: Oxford, 1982; Vol. 6, p 763.
(5) Evans, J.; Gao Jingxing, *J. Chem. Soc., Chem. Commun.* **1985**, 39.
(6) Salter, I. D.; Stone, F. G. A. *J. Organomet. Chem.* **1984**, *260*, C71.
(7) Freeman, M. J.; Green, M.; Orpen, A. G.; Salter, I. D.; Stone, F. G. A. *J. Chem. Soc., Chem. Commun.* **1983**, 1332.
(8) Howard, J. A. K.; Salter, I. D.; Stone, F. G. A. *Polyhedron* **1984**, *3*, 567.
(9) Bonnett, J.-J.; Lavinge, G.; Papageorgiou, F. *Inorg. Chem.* **1984**, *23*, 609.
(10) Bruce, M. I.; Nicholson, B. K. *J. Organomet. Chem.* **1983**, *252*, 243.
(11) Bruce, M. I.; Nicholson, B. K. *Organometallics* **1984**, *3*, 101.
(12) Bateman, L. W.; Green, M.; Mead, K. A.; Mills, R. M.; Salter, I. D.; Stone, F. G. A.; Woodward, P. *J. Chem. Soc., Dalton. Trans.* **1983**, 2599.
(13) Bruce, M. I.; Shawkataly, O. B.; Nicholson, B. K. *J. Organomet. Chem.* **1984**, *275*, 223.
(14) Bruce, M. I.; Horn, E.; Shawkataly, O. B.; Snow, M. R. *J. Organomet. Chem.* **1985**, *280*, 289.
(15) Bruce, M. I.; Shawkataly, O. B.; Nicholson, B. K. *J. Organomet. Chem.* **1985**, *286*, 427.
(16) Salter, I. D. *J. Organomet. Chem.* **1985**, *295*, C17.
(17) Braunstein, P.; Rose, J.; Dedieu, A.; Dusausoy, Y.; Maugeot, J.-P.; Tiripicchio, A.; Tiripicchio-Camellini, M. *J. Chem. Soc., Dalton Trans.* **1986**, 225.

0276-7333/87/2306-0794$01.50/0

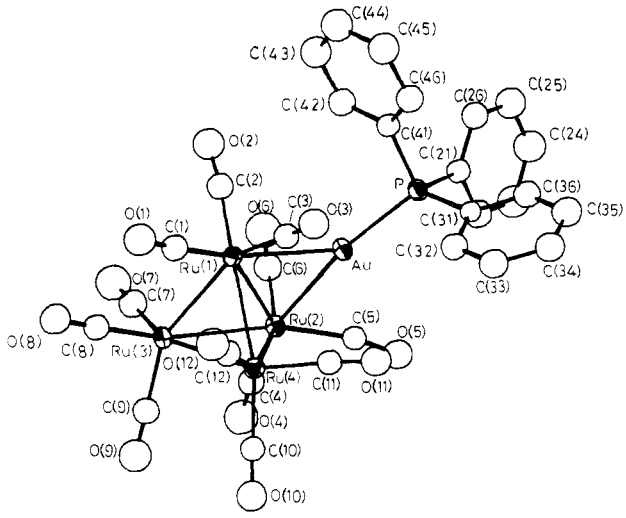

Figure 1. $H_3Ru_4(CO)_{12}AuPPh_3$ showing the atom numbering scheme with thermal ellipsoids drawn at the 40% probability level. H atoms have been omitted for clarity.

instruments. $^{31}P\{^1H\}$ NMR spectra were collected on a Bruker AM-360 spectrometer at 145.8 MHz; chemical shifts are given with reference to 85% H_3PO_4.

Crystallographic Structure of $H_3Ru_4(CO)_{12}AuPPh_3$. Suitable air-stable crystals were obtained from CH_2Cl_2/petroleum ether (40–60 °C) by vapor diffusion at room temperature and mounted in thin-wall glass capillaries. Preliminary photographic X-ray examination established the crystal system and approximate cell dimensions. With use of a room-temperature crystal (0.4 × 0.3 × 0.1 mm), accurate cell dimensions were obtained by least-squares refinement of 25 accurately centered reflections using an Enraf-Nonius CAD4 diffractometer equipped with Mo radiation and graphite monochromator. No significant variation was noted in the three check reflections during the data collection. An empirical absorption correction was applied to the data by using the ψ scan data from several $\chi > 80°$ reflections (transmission 99.6 (max) and 40.5% (min)). The intensity data were converted to F_o after correction for Lorentz and polarization effects. Additional details of the data collection are summarized in Table I.

Structure Solution and Refinement. There were no systematic absences and the space group is either $P1$ or $P\bar{1}$. The normalized structure factors suggested a centric distribution and the centrosymmetric space group $P\bar{1}$ (No. 2) was confirmed by the subsequent analysis. The centrosymmetric direct methods strategy in SHELX (EEES)[18] with $E_{min} = 1.60$ revealed the position of the Ru and Au atoms from the solution with the highest figure of merit. Repeated structure factor calculations and electron density syntheses located the remaining non-hydrogen atoms. These atoms were refined in stages by using first isotropic and later anisotropic thermal parameters for Au, Ru, and P atoms. The difference electron density synthesis indicated several phenyl H atoms, and all five per phenyl group were introduced into the model with calculated positions (d(C–H) = 0.95 Å) and a common refined isotropic temperature factor. Least-squares refinement reduced R to 0.036 at which stage four reflections thought to be subject to extinction ($\bar{1}10$, $\bar{1}01$, 101, 011) were omitted and the difference electron density map examined for possible hydride atom positions. Of the three largest plausible features, two were in suitable positions for edge-bridging H atoms (0.59 e Å^{-3}) whereas the third was in a chemically unreasonable position. Of the several other weak features observed in the map a number were unreasonably close to other atoms and only one peak (0.45 e Å^{-3}) was located both near the metal cluster and at suitable bonding distances from the Ru atoms (μ_3-H). Support for these three peaks being associated with the hydride atoms came from (i) Ru–Ru distances, (ii) Ru–Ru–C angles, and (iii) C···C nonbonded distances in carbonyls (all three being increased by the presence of H atoms). These three hydrogen atoms were introduced into the model with a fixed temperature factor (0.08 Å^2) and refined coordinates.

The maximum shift/error in the final cycle of refinement was 0.28, and a difference electron density synthesis showed all features in the range +1.25 to −1.06 e Å^{-3}. The final R value is 0.0347 for 5326 observed reflections ($F > 3\sigma(F)$) [197 parameters, anisotropic (Au, Ru, P) and isotropic (O, C, H) atoms, rigid C_6 groups (d(C–C) = 1.395 Å), calculated phenyl H atom positions (d(C–H) = 0.95 Å)]. Atomic scattering factors for neutral atoms and anomalous dispersion corrections were taken from ref 20 (Au, Ru) and SHELX[18] (P, O, C, H). All calculations were performed by using the programs in ref 18 and 19. Final atomic coordinates are listed in Table II, and Figure 1 shows the atom numbering scheme used. Interatomic distances and angles are listed in Tables III and IV,

Table II. Atomic Coordinates and Isotropic Temperature Factors (×10^3) for $H_3Ru_4(CO)_{12}AuPPh_3$

	x	y	z	U, Å^2
Au	0.19455 (3)	0.16677 (2)	0.26092 (2)	33.8 (1)[a]
Ru(1)	0.17987 (6)	0.39346 (4)	0.23636 (3)	32.2 (3)[a]
Ru(2)	0.35182 (6)	0.20312 (4)	0.15767 (3)	32.0 (3)[a]
Ru(3)	0.35216 (6)	0.42772 (4)	0.12657 (3)	34.1 (3)[a]
Ru(4)	0.07215 (6)	0.27347 (5)	0.06404 (3)	33.0 (3)[a]
P	0.1144 (2)	0.0820 (1)	0.3481 (1)	32.9 (7)[a]
C(1)	0.1026 (9)	0.5397 (7)	0.2343 (5)	50.6 (18)
O(1)	0.0523 (7)	0.6309 (6)	0.2362 (4)	75.7 (18)
C(2)	0.2977 (9)	0.4545 (7)	0.3499 (5)	50.8 (19)
O(2)	0.3733 (7)	0.4975 (6)	0.4185 (4)	74.2 (17)
C(3)	0.0059 (9)	0.3382 (7)	0.2536 (4)	46.3 (17)
O(3)	−0.1058 (7)	0.3177 (5)	0.2632 (4)	67.9 (16)
C(4)	0.4762 (9)	0.1752 (7)	0.0860 (5)	51.5 (19)
O(4)	0.5512 (8)	0.1475 (6)	0.0414 (4)	86.9 (20)
C(5)	0.3144 (8)	0.0369 (6)	0.1457 (4)	42.0 (16)
O(5)	0.3002 (6)	−0.0644 (5)	0.1257 (3)	61.6 (15)
C(6)	0.5052 (10)	0.2349 (7)	0.2586 (5)	57.1 (21)
O(6)	0.6009 (9)	0.2555 (7)	0.3217 (5)	93.6 (22)
C(7)	0.5466 (10)	0.4758 (7)	0.1929 (5)	57.1 (20)
O(7)	0.6670 (9)	0.5078 (7)	0.2342 (5)	94.0 (22)
C(8)	0.3083 (9)	0.5858 (7)	0.1298 (5)	48.8 (18)
O(8)	0.2851 (7)	0.6840 (5)	0.1340 (4)	69.0 (16)
C(9)	0.4056 (9)	0.3846 (7)	0.0236 (5)	51.4 (19)
O(9)	0.4344 (8)	0.3607 (6)	−0.0398 (4)	78.4 (18)
C(10)	0.0339 (8)	0.2136 (6)	−0.0572 (4)	44.5 (17)
O(10)	0.0075 (7)	0.1816 (5)	−0.1282 (4)	68.1 (16)
C(11)	−0.0482 (8)	0.1504 (6)	0.0690 (4)	44.7 (17)
O(11)	−0.1189 (7)	0.0710 (5)	0.0697 (4)	67.6 (16)
C(12)	−0.0776 (9)	0.3774 (7)	0.0670 (5)	50.6 (19)
O(12)	−0.1742 (8)	0.4389 (6)	0.0682 (4)	81.6 (19)
C(21)	0.2378 (5)	−0.0145 (4)	0.3933 (3)	40.9 (16)
C(22)	0.2919 (5)	−0.1058 (4)	0.3386 (3)	56.6 (20)
C(23)	0.3776 (5)	−0.1884 (4)	0.3695 (3)	76.5 (27)
C(24)	0.4093 (5)	−0.1797 (4)	0.4550 (3)	75.7 (27)
C(25)	0.3552 (5)	−0.0883 (4)	0.5097 (3)	67.6 (24)
C(26)	0.2694 (5)	−0.0057 (4)	0.4789 (3)	50.9 (19)
C(31)	−0.0623 (4)	−0.0073 (4)	0.3040 (3)	32.4 (14)
C(32)	−0.1693 (4)	0.0204 (4)	0.2403 (3)	52.8 (19)
C(33)	−0.3061 (4)	−0.0463 (4)	0.2052 (3)	62.8 (22)
C(34)	−0.3359 (4)	−0.1407 (4)	0.2338 (3)	63.6 (22)
C(35)	−0.2289 (4)	−0.1684 (4)	0.2975 (3)	64.9 (23)
C(36)	−0.0921 (4)	−0.1017 (4)	0.3326 (3)	52.7 (19)
C(41)	0.0939 (5)	0.2047 (4)	0.4370 (3)	39.0 (15)
C(42)	0.2098 (5)	0.2945 (4)	0.4766 (3)	53.2 (19)
C(43)	0.1982 (5)	0.3932 (4)	0.5434 (3)	69.0 (24)
C(44)	0.0707 (5)	0.4020 (4)	0.5706 (3)	73.0 (26)
C(45)	−0.0452 (5)	0.3122 (4)	0.5309 (3)	69.6 (24)
C(46)	−0.0336 (5)	0.2135 (4)	0.4642 (3)	52.7 (19)
H(1)	0.2178 (91)	0.1773 (71)	0.0683 (49)	80.0
H(2)	0.1963 (91)	0.3986 (69)	0.0472 (48)	80.0
H(3)	0.3488 (91)	0.3816 (70)	0.2154 (49)	80.0

[a] Equivalent isotropic temperature factor from anisotropic atom $U_{eq} = {}^1/_3$ trace U.

(18) Sheldrick, G. M. SHELX76, Program for Crystal Structure Determination; University of Cambridge: Cambridge, 1976.

(19) (a) Johnson, C. K., ORTEP, ORNL-3794; Oak Ridge National Laboratory; Oak Ridge, TN, 1965. (b) Motherwell, W. D. S.; Clegg, W. PLUTO, Program for Plotting Molecular and Crystal Structures; Universities of Cambridge and Göttingen: Cambridge and Göttingen 1978.

(20) *International Tables for X-ray Crystallography*; Kynoch Press: Birmingham, England, 1974; Vol. 4, pp 99–101, 149–150.

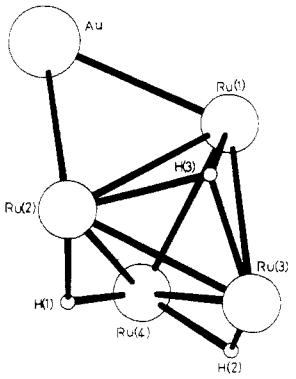

Figure 2. Ru_4Au metal core in $H_3Ru_4(CO)_{12}AuPPh_3$ showing the location of the hydride atoms. Atoms have been drawn with arbitrary size.

Table III. Selected Bond Distances (Å) for $H_3Ru_4(CO)_{12}AuPPh_3$

Ru(1)–Ru(2)	2.965 (1)	Au–Ru(1)	2.809 (1)
Ru(1)–Ru(3)	2.912 (1)	Au–Ru(2)	2.723 (1)
Ru(1)–Ru(4)	2.780 (1)	Au–P	2.305 (2)
Ru(2)–Ru(3)	2.838 (1)	P–C(21)	1.809 (4)
Ru(2)–Ru(4)	2.956 (1)	P–C(31)	1.818 (4)
Ru(3)–Ru(4)	2.956 (1)	P–C(41)	1.814 (4)
Ru–C(min)	1.863 (8)	C–O(min)	1.124 (8)
Ru–C(max)	1.926 (7)	C–O(max)	1.172 (10)
Ru–C(mean)	1.89 (2)	C–O(mean)	1.15 (1)
H(1)–Ru(2)	1.66 (8)	H(3)–Ru(1)	1.72 (8)
H(1)–Ru(4)	1.77 (8)	H(3)–Ru(2)	2.03 (8)
H(2)–Ru(3)	1.67 (8)	H(3)–Ru(3)	1.78 (8)
H(2)–Ru(4)	2.01 (8)		

respectively. Tables of anisotropic thermal parameters, calculated hydrogen positions and observed and calculated structure factors are available (see supplementary material).

Preparation of $H_3Ru_4(CO)_{12}MPR_3$. The bimetallic pentanuclear clusters $[H_3Ru_4(CO)_{12}MPR_3]$ (**1a**,[6] M = Au, R = Ph; **2a**,[16] M = Cu, R = Ph) were prepared by previously reported procedures under a nitrogen atmosphere. Reaction of $[N(PPh_3)_2][H_3Ru_4(CO)_{12}]$ with $AuPPh_3Cl$ and $[Cu(MeCN)_4]PF_6/PPh_3$ yielded **1a** and **2a**, respectively. The analogous complexes **2b** (M = Cu, R = o-MeC_6H_4) and **2c** (M = Cu, R = p-MeC_6H_4) have also been prepared as air-stable, red crystalline solids in yields of 72% and 76%, respectively. The compounds were purified by crystallization from CH_2Cl_2–petroleum ether (bp 40–60 °C).

2b: IR (ν(CO), cyclohexane) 2085 m, 2049 vs, 2024 vs, 2007 m, 1994 s, 1985 m, 1964 w, 1950 w cm^{-1}. NMR spectra: ^1H (CD_2Cl_2) δ 7.0 (m, 4 H, C_6H_4), 2.7 (s, 3 H, CH_3), −17.75 (d, 1 H, J_{PH} = 11 Hz); $^{31}P\{^1H\}$ (CD_2Cl_2) δ −5.79. Anal. Calcd for $C_{33}H_{24}O_{12}CuPRu_4$: C, 35.7; H, 2.2. Found: C, 35.6; H, 2.1. **2c**: IR (ν(CO), cyclohexane) 2085 m, 2049 vs, 2024 vs, 2006 m, 1994 m, 1985 m, 1963 w, 1949 w cm^{-1}. NMR spectra: ^1H (CD_2Cl_2) δ 7.3 (m, 4 H, C_6H_4), 2.4 (s, 3 H, CH_3), −17.65 (d, 1 H, J_{PH} = 11 Hz); $^{31}P\{^1H\}$ (CD_2Cl_2) δ 9.81. Anal. Calcd for $C_{33}H_{24}O_{12}CuPRu_4$: C, 35.7; H, 2.2. Found: C, 35.5; H, 2.1.

Spectroscopic Studies. $H_3Ru_4(CO)_{12}MPR_3$ (1×10^{-5} mol, 0.029 M) in CD_2Cl_2 was analyzed by ^1H NMR (100 MHz) at 31 °C. The effect of adding PR_3 to this solution on the hydride resonance was monitored after the addition of each aliquot of phosphine. The effect of adding PR_3 to a CH_2Cl_2 solution of $H_3Ru_4(CO)_{12}MPR_3$ on the ν(CO) bands of the cluster species was examined by IR spectroscopy. Variable-temperature ^1H (360 MHz) and $^{31}P\{^1H\}$ (145.8 MHz) NMR studies were performed on mixtures of known stoichiometry of $H_3Ru_4(CO)_{12}MPR_3$ and PR_3, in CD_2Cl_2, $CDCl_3$, or toluene-d_8. All systems were tested for reversibility.

Results

The $H_3Ru_4(CO)_{12}AuPPh_3/PPh_3$ System. The ^1H NMR spectrum of a 2:1 mixture of $H_3Ru_4(CO)_{12}AuPPh_3/PPh_3$ in $CDCl_3$ at 210 K consisted of three signals in addition to that of the heterometallic cluster **1**[6] at δ −17.70. These were consistent with the low-temperature resonances of $[H_3Ru_4(CO)_{12}]^-$ previously assigned[21] as being due to the two isomeric forms of the anion. At 278 K the anion signals coalesced resulting in a broad averaged peak at δ −17.10, in addition to the unchanged resonance at δ −17.70. Elevation in temperature (in toluene-d_8) caused coalescence at 312 K and the appearance of two new signals at δ −17.35 and −16.73 at 363 K. The $^{31}P\{^1H\}$ NMR spectrum of this mixture in the range 215–305 K exhibited two resonances at +68.3 and +44.5 ppm consistent with the previously reported values for **1**[6] and $[Au(PPh_3)_2]^+$,[22] respectively. The signal of the latter broadens more than the former with increasing temperature, indicating that the cationic species undergoes exchange, possibly with free phosphine, at a rate faster than the exchange between the cation and the mixed-metal cluster. However, at 305 K broadening of the resonance due to this cluster is also observed. This study indicates an essentially stoichiometric reaction between **1a** and PPh_3 leading to the formation of $[Au(PPh_3)_2]^+$ as shown in eq 1.

$$H_3Ru_4(CO)_{12}AuPPh_3 + PPh_3 \rightleftharpoons [Au(PPh_3)_2]^+[H_3Ru_4(CO)_{12}]^- \quad (1)$$

Table IV. Selected Bond Angles (deg) for $H_3Ru_4(CO)_{12}AuPPh_3$

Ru(1)–Ru(2)–Ru(3)	60.2 (1)	Ru(1)–Ru(3)–Ru(4)	56.5 (1)
Ru(2)–Ru(3)–Ru(1)	62.1 (1)	Ru(3)–Ru(4)–Ru(1)	60.9 (1)
Ru(3)–Ru(1)–Ru(2)	57.7 (1)	Ru(4)–Ru(1)–Ru(3)	62.5 (1)
Ru(1)–Ru(2)–Ru(4)	56.0 (1)	Ru(2)–Ru(3)–Ru(4)	61.3 (1)
Ru(2)–Ru(4)–Ru(1)	62.2 (1)	Ru(3)–Ru(4)–Ru(2)	57.4 (1)
Ru(4)–Ru(1)–Ru(2)	61.8 (1)	Ru(4)–Ru(2)–Ru(3)	61.3 (1)
Ru(1)–Au–Ru(2)	64.8 (1)	Au–Ru(1)–Ru(3)	113.9 (1)
Au–Ru(2)–Ru(1)	59.0 (1)	Au–Ru(1)–Ru(4)	87.1 (1)
Ru(2)–Ru(1)–Au	56.2 (1)	Au–Ru(2)–Ru(3)	119.2 (1)
		Au–Ru(2)–Ru(4)	85.3 (1)
P–Au–Ru(1)	134.3 (1)		
P–Au–Ru(2)	159.9 (1)		
Au–P–C(21)	116.2 (2)	C(21)–P–C(31)	103.6 (2)
Au–P–C(31)	117.3 (2)	C(21)–P–C(41)	106.0 (2)
Au–P–C(41)	106.9 (2)	C(31)–P–C(41)	105.9 (2)
Ru–C–O(min)	167.5 (6)		
Ru–C–O(max)	179.6 (6)		
Ru–C–O(mean)	176 (3)		

The $H_3Ru_4(CO)_{12}CuPPh_3/PPh_3$ System. The effect of adding PPh_3 to a solution of **2a**, on the hydride resonance of the ^1H NMR, is illustrated in Figure 3a; this shows the chemical shift (δ, relative to Me_4Si) as a function of PPh_3 concentration. A discontinuity is observed when $[PPh_3]/[\mathbf{2a}] = 2$, indicating the establishment of the equilibrium shown in eq 2. The dynamics of the equilibrium were studied by variable-temperature ^1H (274–330 K) and ^{31}P (238–329 K) NMR analyses of a 1:1 solution mixture of PPh_3 and **2a**, both at 0.029 M. The hydride region of the ^1H spectrum at 274 K contains a doublet at δ −17.62 (J_{PH} = 11 Hz) assigned to **2a**[6] and a singlet at δ −17.10 due to the anionic species $[H_3Ru_4(CO)_{12}]^-$.[21] With increasing temperature line broadening is apparent; loss of phosphorus coupling in the resonance due to **2a** occurs at 299 K, and at 330 K a broad averaged signal is observed

$$H_3Ru_4(CO)_{12}CuPPh_3 + 2PPh_3 \rightleftharpoons [Cu(PPh_3)_3]^+[H_3Ru_4(CO)_{12}]^- \quad (2)$$

(21) Koepke, J. W.; Johnson, J. R.; Knox, S. A. R.; Kaesz, H. J. *J. Am. Chem. Soc.* **1975**, *97*, 3947.
(22) Vollenbroek, F. A.; van den Berg, J. P.; van der Velden, J. W. A.; Bour, J. J. *Inorg. Chem.* **1980**, *19*, 2685.

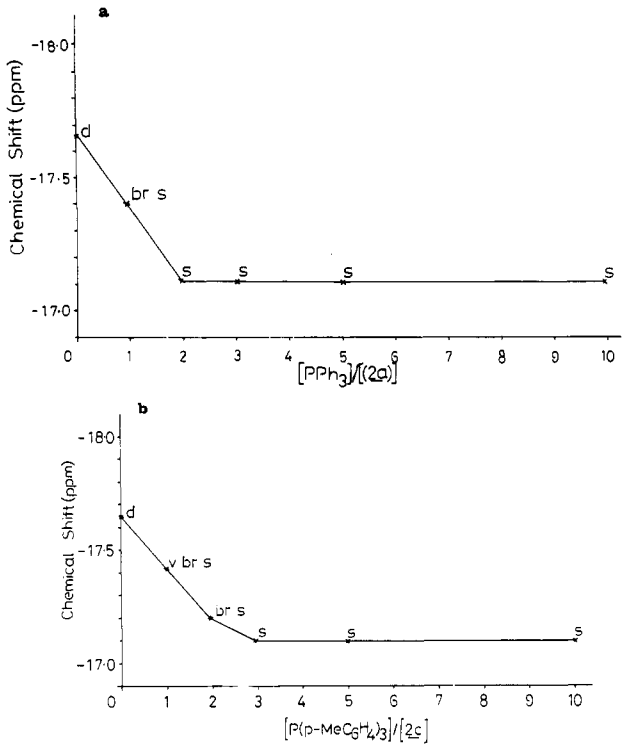

Figure 3. ^1H chemical shift of the hydride resonances observed for mixtures of (a) **2a** and PPh_3 and (b) **2c** and $P(p\text{-}MeC_6H_4)_3$ (d = doublet; s = singlet; br = broad).

at δ −17.43, indicating rapid exchange of the $CuPPh_3$ moiety. From the integration and line width of the hydride signals at 285 K the equilibrium and rate constant (at these concentrations) for the process at this temperature have been estimated as 1300 M^{-2} and 30 s^{-1}, respectively. [The equilibrium constant was determined by using

	$H_3Ru_4(CO)_{12}CuPPh_3$ +	$2PPh_3$ ⇌	$[Cu(PPh_3)_3][H_3Ru_4(CO)_{12}]$
initial concn	a	$2a$	0
concn at equil	$a - x$	$2(a - x)$	x

$$K_{eq} = x/[(a - x)[2(a - x)]^2]$$

x and $(a - x)$ were determined from the integration ratio of the hydride resonances in the proton NMR spectra at 285 K. The rate constant was estimated near the slow-exchange limit assuming Lorentzian line shape. $k \cong 1/T_2' = \pi\Delta\nu_{1/2}$ where $\Delta\nu_{1/2}$ is the line width at half-height at exchange.] The ^{31}P spectrum of a 2:1 solution mixture of PPh_3 and **2a** at 305 K consisted of a single resonance at δ 1.92 (relative to H_3PO_4 (external)) which apart from shifting to lower frequency (0.3 Hz/°C) and slight sharpening, is unchanged at 175 K. This chemical shift corresponds to those observed for $[Cu(PPh_3)_3][BF_4]$[23] and $[Cu(PPh_3)_3][MCo_3(CO)_{12}]$.[17] For the 3:1 mixture of PPh_3/**2a**, the ^{31}P resonance was observed at δ 0.66, indicating the presence of an equilibrium involving the CuL_n^+ species. This is consistent with the previously reported investigations of the behavior of tertiary phosphine complexes of copper(I) in solution.[24-26]

The $H_3Ru_4(CO)_{12}CuP(p\text{-}MeC_6H_4)_3/P(p\text{-}MeC_6H_4)_3$ System. The effect of adding $P(p\text{-}MeC_6H_4)_3$ to a solution of $H_3Ru_4(CO)_{12}CuP(p\text{-}MeC_6H_4)_3$, on the ^1H NMR (100 MHz) of the hydride resonance, is illustrated in Figure 3b. As with the PPh_3 system, the dynamics of the equilibrium shown in eq 3 were studied by variable-temperature ^1H

$$H_3Ru_4(CO)_{12}CuP(p\text{-}MeC_6H_4)_3 + 2P(p\text{-}MeC_6H_4)_3 \rightleftharpoons [Cu(P(p\text{-}MeC_6H_4)_3)_3]^+ + [H_3Ru_4(CO)_{12}]^- \quad (3)$$

(265–330 K) and ^{31}P (250–318 K) NMR analyses of a 1:1 solution mixture of $P(p\text{-}MeC_6H_4)_3$/**2c**, both at 0.029 M. The hydride region of the ^1H spectrum at 265 K contains a doublet at δ −17.67 (J_{PH} = 12.4 Hz) assigned to the complex **2c** and the anion resonance at δ −17.10. The presence of these two species is also apparent from the methyl region of the spectrum that exhibits two singlet resonances at δ 2.31 and 2.41, the latter being due to the cluster **2c**. Line broadening is apparent with increasing temperature, until at 330 K broad-averaged signals are observed at δ −17.43 and 2.37.

The equilibrium and rate constants were estimated as 174 M^{-2} and 30 s^{-1}, respectively, under the same conditions as those determined for the PPh_3 system. The fluxional process is best described by the variable-temperature ^{31}P spectra of this mixture. The spectrum at 250 K indicates the presence of free phosphine in addition to the species $[Cu(P(p\text{-}MeC_6H_4)_3)_3]^+$ at δ 0.05 and **2c** at δ 9.32. The spectrum at 285 K indicates that the exchange between the copper cationic species and free phosphine proceeds at a faster rate than that between the cation and the cluster **2c**. When the mixture is warmed to 318 K, the signals of the latter two species coalesce to give an averaged signal at δ 9.66. The more extensive broadening of the resonance due to the copper cationic species may be attributed to the quadrupolar effect of the metal atom.

The $H_3Ru_4(CO)_{12}CuP(o\text{-}MeC_6H_4)_3/P(o\text{-}MeC_6H_4)_3$ System. When $P(o\text{-}MeC_6H_4)_3$ is added to a solution of **2b**, appreciable formation of the anion $[H_3Ru_4(CO)_{12}]^-$ does not occur until a ligand/cluster ratio of approximately 40:1 is achieved. This is supported by IR studies. No line broadening was observed in the variable-temperature ^1H (235–332 K) and $^{31}P\{^1H\}$ (194–303 K) NMR spectra of a 2:1 mixture of $P(o\text{-}MeC_6H_4)_3$/**2b**. The ^1H spectra consisted of a doublet at δ −17.62 ± 0.04, and in the ^{31}P spectra, two singlets were apparent at δ −7.5 and −29.5 due to **2b** and $P(o\text{-}MeC_6H_4)_3$, respectively.

Discussion

The Structure of $H_3Ru_4(CO)_{12}AuPPh_3$. The structure consists of discrete molecules, and one is shown in Figure 1. The ruthenium atoms form an approximate tetrahedron with the gold atom bridging over the Ru(1)–Ru(2) edge and forming an almost planar Ru(1)Ru(2)Ru(3)Au group. (The angle between the Ru(1)Ru(2)Ru(3) and Ru(1)Ru(2)Au planes is 0.5(1)°.) The Ru–Ru distances are in accord with earlier structures with the shortest distance (2.780 (1) Å), as expected, not involved with the hydride atoms. Each Ru atom is bonded to three terminal CO groups with no bridging or semibridging groups. The Au–Ru distances are unequal (difference 0.086 (2) Å); the phosphorus of the triphenylphosphine residue is positioned unsymmetrically with respect to Ru(1) and Ru(2) and displaced from the Ru(1)Ru(2)Au plane (0.22 (1) Å). The positions of the hydride atoms with respect to the skeleton are shown in Figure 2; these differ from the arrangement in $H_4Ru_4(CO)_{12}$.[27] Two of the hydride atoms show edge bridging (μ_2-H, Ru–H–Ru angles = 119 (5) and 106 (4)°), and the third is positioned over the Ru(1)Ru(2)Ru(3) face (μ_3-H, distance from the face = 0.7 (1) Å). The triphenylphosphine and carbonyl group

(23) Levason, W.; Spicer, M. D., personal communication.
(24) Muetterties, E. L.; Alegranti, C. W. *J. Am. Chem. Soc.* **1970**, *92*, 4114.
(25) Lippard, S. J.; Mayerle, J.-J. *Inorg. Chem.* **1972**, *11*, 753.
(26) Gulliver, D. J.; Levason, W.; Webster, M. *Inorg. Chim. Acta* **1981**, *52*, 153.
(27) Wilson, R. D.; Wu, S. M.; Lowe, R. A.; Bau, R. *Inorg. Chem.* **1978**, *17*, 1271.

bond lengths and angles are unexceptional.

A considerable number of bimetallic clusters of gold and ruthenium have been characterized by X-ray crystallography and four examples of Ru_4 clusters have been reported. The $H_3Ru_4(CO)_{12}AuPPh_3$ has a ruthenium skeleton similar to that of $H_4Ru_4(CO)_{12}$.[27] In the latter structure the six Ru–Ru distances can be categorized into two groups: the four longer lengths which are believed to be hydride-bridged, Ru–Ru(average) = 2.9499 Å, and the two shorter lengths, Ru–Ru(average) = 2.7860 Å. Thus, by comparison in the present molecule, the Ru–Ru length bridged by the $AuPPh_3$ moiety is 0.015 Å greater than the averaged hydride-bridged Ru–Ru distance. There are no other significant bond length differences between the two structures. The edge-bridging Au bonding is unlike that in the carbide compound $HRu_4C(CO)_{12}AuPPh_3$[28] where there is a "butterfly" Ru_4 skeleton with the Au atom located over the "wingtips". Rather the title compound is analogous to the osmium compound $H_3Os_4(CO)_{12}AuPEt_3$[29] although in this example not surprisingly the H atoms were not located by the diffraction experiment.

Fluxional Decapping of $H_3Ru_4(CO)_{12}MPAr_3$. Recently, it has been reported[17] that the trimetallic pentanuclear clusters $MCo_3(CO)_{12}[\mu_3\text{-}CuPPh_3]$ (M = Fe, Ru) react with PPh_3 to give the ionic cluster species $[Cu(PPh_3)_3][MCo_3(CO)_{12}]$ whereas the compound $RuCo_3(CO)_{12}[\mu_3\text{-}AuPPh_3]$ reacts with PPh_3 to give $[Au(PPh_3)_2][RuCo_3(CO)_{12}]$. Clearly the reactivity of both clusters is fast on a synthetic time scale. However, the present NMR study has indicated a distinct difference in rate between $[AuPPh_3]$ and $[CuPPh_3]$ with this type of reactivity. Thus, the rate of $[MPPh_3]$ exchange is much faster for the ruthenium–copper complex than for the ruthenium–gold cluster, despite the former requiring the reversible dissociation of a higher connectivity metal center. In both studies the strong preference for the formation of $[Cu(PPh_3)_3]^+$ is observed. For the complexes **2a** and **2c** whose phosphines do not differ in cone angle (145°) the rate constant for the decapping process was identical. Increasing the steric bulk of the phosphine to that in **2b** (194°) retards the intermolecular exchange process. Clearly the formation of $[Cu(P(o\text{-}MeC_6H_4)_3)_n]^+$ (n = 2 or 3) is sterically unfavorable. Despite the identical rate constant for the clusters **2a** and **2c**, the equilibrium constant for the former was approximately sevenfold greater. This corresponds to a difference in ΔG for ion formation of −5 kJ mol^{-1}. Attempts may be made to rationalize this very small energy difference in terms of the electron-donating power of the phosphine, $PPh_3 < P(p\text{-}MeC_6H_4)_3$.[30] It has been shown by Evans and Mingos[31] that for the $AuPPh_3$ fragment, the p_x and p_y orbitals are relatively high lying and cannot accept electron density as effectively as $CuPPh_3$; hence the latter favoring a face-capping mode of binding to the Ru_4 cluster. In comparison with $CuPPh_3$, the more electron-donating phosphine of $CuP(p\text{-}MeC_6H_4)_3$ causes a raising of the p_x and p_y orbitals and therefore reduces their tendency to accept electron density from the cluster. Furthermore, enhanced stabilization of the cationic species by the more electron-donating phosphine would be anticipated. These theoretical considerations are, however, in contrast to the experimental evidence which indicates that the $CuP(p\text{-}MeC_6H_4)_3$ favors cluster binding, although the energy difference for the two phosphines is extremely small.

Acknowledgment. We thank the SERC for financial support (ACS), Dr. M. B. Hursthouse for the X-ray data collection by the SERC/QMC Crystallographic Service, Johnson Matthey Ltd. for the loan of ruthenium chloride, and Mrs. J. M. Street for some of the NMR spectra.

Registry No. **1a**, 87855-06-9; **2a**, 89506-28-5; **2b**, 106781-75-3; **2c**, 106781-76-4; $[Au(PPh_3)_2]^+[H_3Ru_4(CO)_{12}]^-$ (isomer 1), 106781-77-5; $[Au(PPh_3)_2]^+[H_3Ru_4(CO)_{12}]^-$ (isomer 2), 106781-78-6; $[Cu(PPh_3)_3]^+[H_3Ru_4(CO)_{12}]^-$ (isomer 1), 106781-79-7; $[Cu(PPh_3)_3]^+[H_3Ru_4(CO)_{12}]^-$ (isomer 2), 106781-81-1; $[Cu(P(p\text{-}MeC_6H_4)_3]^+[H_3Ru_4(CO)_{12}]^-$ (isomer 1), 106781-80-0; $[Cu(P(p\text{-}MeC_6H_4)_3)_3]^+[H_3Ru_4(CO)_{12}]^-$ (isomer 2), 106781-82-2; Cu, 7440-50-8; Au, 7440-57-5; Ru, 7440-18-8; PPh_3, 603-35-0; $P(p\text{-}MeC_6H_4)_3$, 1038-95-5; $P(o\text{-}MeC_6H_4)_3$, 6163-58-2.

Supplementary Material Available: Tables of anisotropic thermal parameters and calculated H-atom positions (2 pages); a listing of observed and calculated structure factors (30 pages). Ordering information is given on any current masthead page.

(28) Cowie, A. G.; Johnson, B. F. G.; Lewis, J.; Raithby, P. R. *J. Chem. Soc., Chem. Commun.* **1984**, 1710.
(29) Johnson, B. F. G.; Kaner, D. A.; Lewis, J.; Raithby, P. R.; Taylor, M. J. *J. Chem. Soc., Chem. Commun.* **1982**, 314.
(30) Tolman, C. A. *Chem. Rev.* **1977**, *77*, 313.
(31) Evans, D. G.; Mingos, D. M. P. *J. Organomet. Chem.* **1982**, *232*, 171.